JACS
JOURNAL OF THE AMERICAN CHEMICAL SOCIETY
Article
pubs.acs.org/JACS

Evidence of Entropy-Driven Bistability through ^{15}N NMR Analysis of a Temperature- and Solvent-Induced, Chiroptical Switching Polycarbodiimide

James F. Reuther[†,‡] and Bruce M. Novak*[,‡]

[†]Department of Chemistry, North Carolina State University, 2620 Yarbrough Drive, Raleigh, North Carolina 27695, United States
[‡]Department of Chemistry and Alan G. MacDiarmid NanoTech Institute, University of Texas Dallas, 800 West Campbell Road, Richardson, Texas 75080, United States

Supporting Information

ABSTRACT: The thermo- and solvo-driven chiroptical switching process observed in specific polycarbodiimides occurs in a concerted fashion with large deviations in specific optical rotation (OR) and CD Cotton effect as a consequence of varying populations of two distinct polymer conformations. These two conformations are clearly visible in the ^{15}N NMR and IR spectra of the ^{15}N-labeled poly(^{15}*N*-(1-naphthyl)-*N*′-octadecylcarbodiimide) (**Poly-3**) and poly(^{15}*N*-(1-naphthyl)-^{15}*N*′-octadecylcarbodiimide) (**Poly-5**). Using van't Hoff analysis, the enthalpies and entropies of switching ($\Delta H_{switching}$; $\Delta S_{switching}$) were calculated for both **Poly-3** and **Poly-5** using the relative integrations of both peaks in the ^{15}N NMR spectra at different temperatures to measure the populations of each state. The chiroptical switching (i.e., transitioning from state A to state B) was found to be an endothermic process (positive $\Delta H_{switching}$) for both **Poly-3** and **Poly-5** in all solvents studied, meaning the conformation correlating with the downfield chemical shift (ca. 148 ppm, state B) is the higher enthalpy state. The compensating factor behind this phenomenon has been determined to be the large increase in entropy in $CHCl_3$ as a result of the switching. Herein, we propose that the increased entropy in the system is a direct consequence of increased disorder in the solvent as the switching occurs. Specifically, the chloroform solvent molecules are very ordered around the polymer chains due to favorable solvent−polymer interactions, but as the switching occurs, these interactions become less favorable and disorder results. The same level of solvent disorder is not achieved in toluene, causing the chiroptical switching process to occur at higher temperatures.

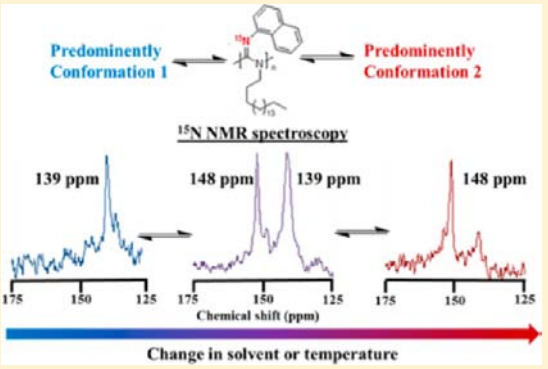

INTRODUCTION

Synthesis and control of molecular switches presents important, significant challenges in designing nanomachines capable of minute changes to the overall primary or secondary structure at the molecular level. Bistability, the presence of two specific molecular structures that can interconvert between one another upon influence from external stimuli, is a necessary attribute in all molecular switches. Various external stimuli have been shown to cause this phenomenon including alterations of photochemical irradiation,[1] solvent,[2] heat,[3] pressure,[4] magnetic/electronic fields,[5] or pH change,[6] with irradiation and heat being the predominant stimuli studied. Chiroptical switches undergo molecular modifications that precisely alter the chirality of the compound in question. The alteration to the molecular structure of the switch can vary from helical inversion[7] to cis−trans isomerization[8] to cyclization[9] and typically can be monitored by polarimetry, electronic circular dichroism (ECD), vibrational circular dichroism (VCD), and Raman spectroscopy.[10] Applying these molecular switch functionalities to macromolecular systems offers possibilities of alterations to self-assembly of the polymer chains in gels,[11] liquid crystals,[12] and Langmuir−Blodgett films.[13] Specific molecular switch functional groups have also been incorporated into several polymer systems including polymethacrylates,[14] polypeptides,[15] DNA,[16] and polyisocyanates[17] to name a few. These systems offer a vast amount of potential applications in the field of materials science.

In addition, formation of optically active, helical macromolecules with an excess single-handed screw sense has been an evergrowing field of interest in the past two decades due to their potential uses as asymmetric polymeric catalyst supports, chiral sensors, polymeric liquid crystals, and/or stationary phases in chiral separations.[18−26] Throughout this time, novel, helical macromolecular scaffolds have emerged including systems such as oligio-[27] and poly(*m*-phenylene ethynylenes),[28,29] polyisocyanates,[30,31] polyisocyanides,[32−34] poly(phenyl acetylenes),[35,36] poly(quinaxoline-2,3-dials),[37,38] and

Received: September 27, 2013
Published: December 6, 2013

   dx.doi.org/10.1021/ja4098803 | *J. Am. Chem. Soc.* 2013, 135, 19292−19303

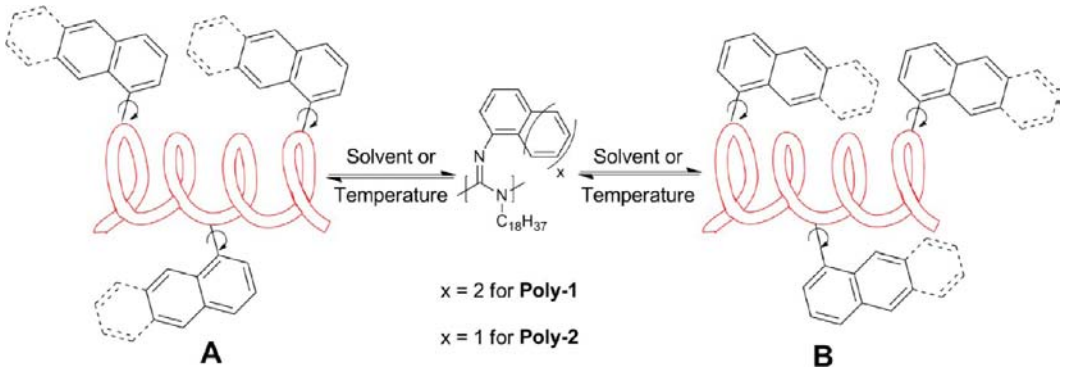

Figure 1. Chiroptical switching property of **Poly-1** and **Poly-2** observed in dilute solutions was hypothesized to be caused by the shutter-like rotation of the aryl pendant group.

polycarbodiimides[39] to name a few. Polycarbodiimides, a relatively young class of helical macromolecules, have been an intense area of interest in the Novak group since the discovery of the controlled "living" Ti(IV)-mediated polymerization of carbodiimides in 1994 due to their attractive properties such as liquid crystallinity,[40,41] high helical inversion barrier,[42] and chiroptical switching.[43−46]

In 2005, Tang et al. reported the first polycarbodiimide possessing reversible solvent- and temperature-induced chiroptical switching in toluene.[45] The achiral monomer was polymerized with the chiral [(*R*)-(3,3′-dibromo-2,2′-binaphthoxy]Ti(IV) di-*tert*-butoxide catalyst to form an optically active polymer with excess single-handed helical sense. The specific optical rotation (OR; [α]) and ECD cotton effect of poly(*N*-(1-anthryl)-*N*′-octadecyl carbodiimide) (**Poly-1**) were able to be modulated reversibly from positive to negative values upon increasing the temperature of the dilute polymer solution above 38.5 °C in toluene. In addition, doping the polymer solution with 10% (v/v) THF or greater caused the specific OR and ECD Cotton effect to exhibit the low negative values observed in pure toluene at high temperatures. **Poly-1**, however, showed no optical temperature dependence in THF or $CHCl_3$, and the ECD Cotton effect remained negative at all temperatures.

Three possible molecular motions were hypothesized to be the cause of this phenomenon including helical inversions, imine inversions, and/or rotation about the N−$C_{anthracene}$ bond. Full racemization of the polymer backbone for **Poly-1** required substantially more energy (ca. 100 h at +80 °C)[42] to occur than the low-energy switching process. The reversibility of the process also contests the possibility that helical inversions play a role since more than four heating/cooling cycles were undergone without any significant racemization occurring. Also, imine configuration interconversions in small molecule analogs have been reported in the range of 20−26 kcal/mol converting to analogous temperatures of 50−180 °C.[47] Coupling the data collected with experimental and theoretical VCD data, Tang et al. ruled out both helical inversions and imine inversions as viable sources for the chiroptical changes observed leaving rotation about the N−C_{aryl} bond in a shutter-like motion as a function of temperature and solvent polarity (Figure 1).[46] Upon influence of solvent or temperature, the aryl groups synchronously reorient themselves to the slightly higher energy state (B) aligning in the same general direction as the helical director. The more polar solvents ($CHCl_3$ or THF) were believed to stabilize a more polar, high-energy state with their signature low negative OR and ECD cotton effects.

Later in 2010, Kennemur et al. reported a new, more versatile polycarbodiimide possessing amplified chiroptical switching properties in numerous different solvents.[43] Poly(*N*-(1-naphthyl)-*N*′-octadecylcarbodiimide) (**Poly-2**) contains the naphthyl pendant group capable of acting as the rotating flap much like the more sterically bulky anthracene moiety. As a result, the optical properties were enhanced with net specific OR deviations of more than 1700° and the ability to switch, i.e., pass from positive OR to negative, in eight different solvents.

The different solvents shown to induce chiroptical switching in **Poly-2** are decisively diverse and include aromatic hydrocarbons (toluene, xylenes, ethylbenzene, propylbenzene), halogenated solvents ($CHCl_3$, 1,2-dichlorobenzene, chlorobenzene), and ethers (THF). Each solvent has varied effects on the chiroptical switching of **Poly-2**, but chloroform, THF, and toluene were found to possess the largest amplitude of chiroptical switching. At first examination of **Poly-1**, the solvent effects on the switching process seem intuitively correlated to the polarity of the solvent, but no such trend exists between the solvent used and the observed switching of **Poly-2**.

Recently, we reported the use of ^{15}N NMR spectroscopy to directly probe the regioregularity of various nitrogen-15-enriched polycarbodiimides.[48,49] All polycarbodiimides wielding two sterically inequivalent pendant groups, i.e., aromatic vs primary aliphatic groups, were discovered to be completely regioregular with the more bulky substituents solely located on the C═N backbone imine nitrogen. **Poly-2** was initially chosen for ^{15}N enrichment to elucidate the regioregularity of asymmetric polycarbodiimides and the presence of two C═N imine stretches in the IR spectrum.

The corresponding monomer was polymerized using the chiral (*R*)-BINOL Ti(IV) diisopropoxide catalyst (**Cat-1**(***R***)) to form poly(^{15}*N*-(1-naphthyl)-*N*-octadecylcarbodiimide) (**Poly-3**) with an excess helical sense. This polymer was found to be completely regioregular as evidence by the single peak present in the ^{15}N NMR spectra in toluene-d_8. This result along with the VT-IR data suggests that examining the imine C═N stretch in the FTIR spectra is not a sufficient handle for regioregularity determination and that the stretch may offer some insight into the switching process.

Herein, we propose a two-state model where the chiroptical switching process is a consequence of two distinct polymer conformations. We report the effect of solvent and temperature on the ^{15}N NMR spectra of **Poly-3** and the newly synthesized, dilabeled poly(^{15}*N*-(1-naphthyl)-^{15}*N*-octadecylcarbodiimide) (**Poly-5**). In addition, the solvent and temperature effects

dx.doi.org/10.1021/ja4098803 | J. Am. Chem. Soc. 2013, 135, 19292−19303

observed in the ^{15}N NMR are compared with the specific OR, ECD, and IR data of **Poly-3**. The synthesis and ^{15}N NMR analysis of poly(^{15}N-(2-naphthyl)-*N*-octadecylcarbodiimide (**Poly-4**) is also reported to compare with the chiroptical switching **Poly-3** and **-5**. The structures of **Poly-3**, **-4**, and **-5** are shown in Figure 2.

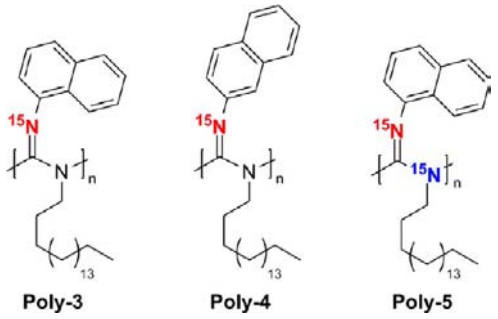

Figure 2. ^{15}N-labeled polycarbodiimides synthesized to further analyze the chiroptical switching process first observed in **Poly-1** and **Poly-2**.

EXPERIMENTAL SECTION

Materials. ^{15}N-labeled ammonium chloride ($^{15}NH_4Cl$, Cambridge Isotope Laboratories, Cambridge, MA), sodium nitrate ($Na^{15}NO_3$, Cambridge Isotope Laboratories, Cambridge, MA), and potassium phthalimide (Cambridge Isotope Laboratories, Cambridge, MA) were purchased as 99% nitrogen-15 enriched and used as received. Deuterated chloroform-*d* (Sigma Aldrich, Milwaukee, MI), THF-d_8 (Sigma Aldrich, Milwaukee, MI), toluene-d_8 (Cambridge Isotope Laboratories, Cambridge, MA), dichloromethane-d_2 (Sigma Aldrich, Milwaukee, MI), and benzene-d_6 (Cambridge Isotope Laboratories, Cambridge, MA) were all purchased as 99.5% deuterated NMR solvents and used as received. Solvents used in polymerizations of carbodiimide monomers were distilled prior to use. All other solvents and reagents were also used as received.

Instrumentation. ^1H NMR spectra were collected on Varian Mercury 400 and 300 MHz NMR spectrometers with Oxford Narrow Bore superconducting magnets. The majority of ^{15}N NMR and ^{13}C NMR spectra were conducted on the Varian Mercury 400 MHz Spectrometer. Variable-temperature ^{15}N NMR spectra for van't Hoff analysis were collected on a new Bruker AVANCE III 500 MHz NMR spectrometer for better resolution. IR spectra were collected on a Jasco model 410 FTIR spectrometer either cast onto a KBr salt plate or pressed into a KBr pellet. Specific OR measurements were conducted on a Jasco P-1050 polarimeter in spectrophotometric-grade solvents purchased from Sigma Aldrich (Milwaukee, MI). Mass spectrometry data was collected by the NCSU Department of Chemistry Mass Spectrometry Facility on the Agilent Technologies 6210 LC-TOF Mass Spectrometer. Molecular weight determination was performed using a Shimadzu Prominence Modular HPLC/GPC system connected to a refractive index (RI) detector relative to a polystyrene

Scheme 1. Synthesis Scheme for Isotopically-Enriched Poly-3 and Poly-5 Starting ^{15}N-Labeled Sodium Nitrate and Potassium Phthalimide

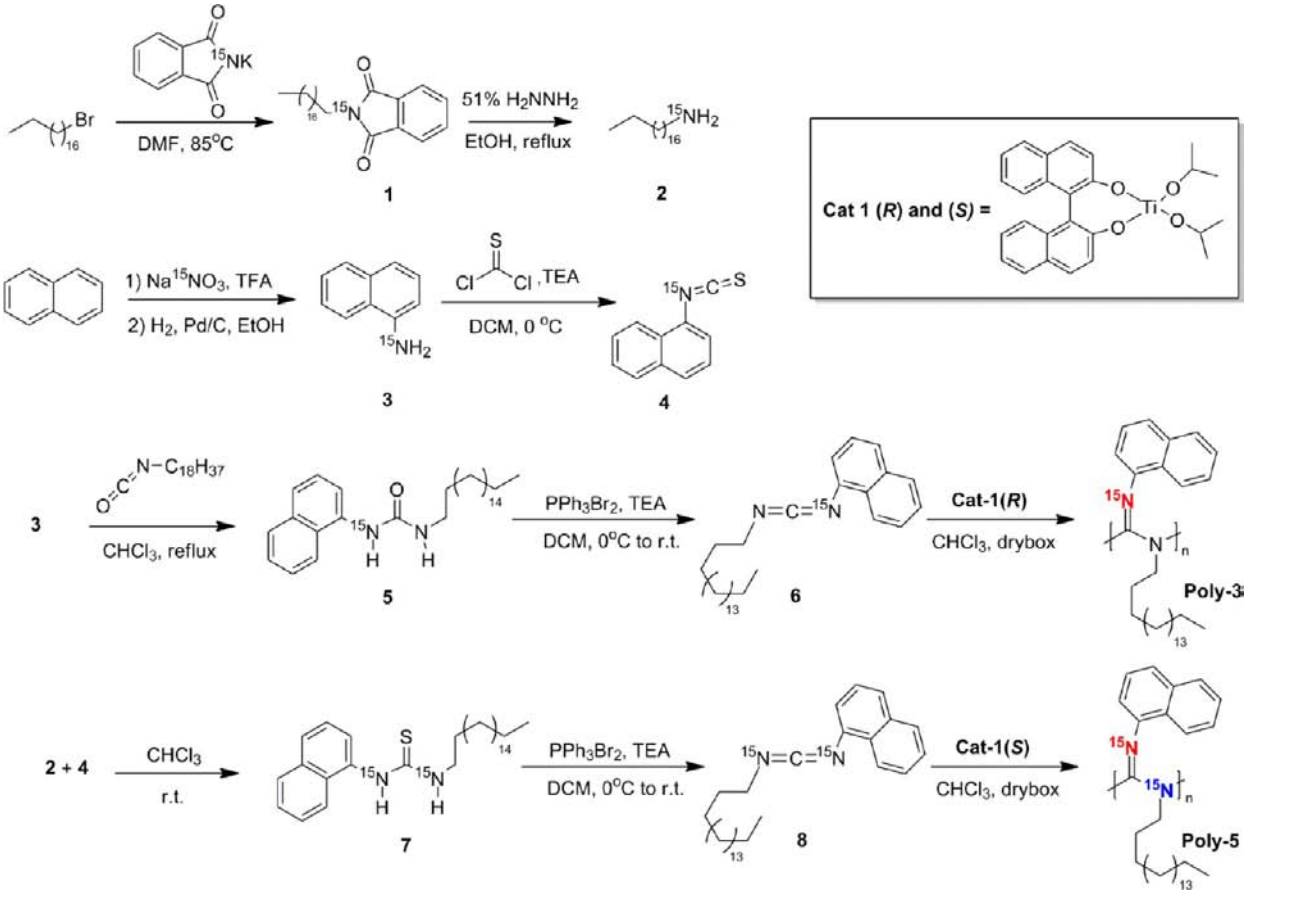

dx.doi.org/10.1021/ja4098803 | J. Am. Chem. Soc. 2013, 135, 19292−19303

standard. A two-column system was employed consisting of an Agilent Mixed-E and Mixed-C column. Polymer samples were dissolved in HPLC-grade chloroform (ca. 1.8 mg/mL) with 0.5% (v/v) *N*,*N*-dimethylethylenediamine added to the sample. Samples were passed through a 0.45 μm PTFE filter prior to injection. The flow rate for all samples was 1.0 mL/min, and the injection volume was 50 μL.

Synthesis of ^{15}N-Enriched Polycarbodiimides. Synthesis schemes for the ^{15}N-labeled **Poly-3** and **Poly-5** are shown in Scheme 1. The procedure for synthesis of the labeled 1-naphthylamine and **Poly-3** was previously reported. Synthesis of the labeled isothiocyanate was carried out using a slightly modified procedure reported by Kai et al.[50] Synthesis the ^{15}*N*-octadecylphthalimide and removal of the phthalimide group was performed following the procedure reported by Wood albeit slightly modified.[51] Synthesis and characterization of the titanium catalysts used for polymerization has been previously reported by Tian et al.[52] **Poly-4** was synthesized using the original protocol for ^{15}N-labeling polycarbodiimides reported by DeSousa and Novak involving amidation of an acid chloride with isotopically enriched ammonium chloride, Hofmann rearrangement to the labeled methyl carbamate, and acidolysis of the carbamate to the amine HCl salt.[48] These reaction procedures, yields, and characterization of compounds can be found in the Supporting Information. Procedures for all unreported reactions are outlined in the section below. For the yields and characterization of all precursor compounds and final ^{15}N-enriched polycarbodiimides, see the Supporting Information.

*Synthesis of ^{15}N-Octadecylphthalimide (**1**).* ^{15}N-enriched potassium phthalimide (1.03 g, 5.56 mmol, 1.0 equiv, 98% isotope enriched) and 1.86 g of 1-bromooctadecane (5.59 mmol, ∼1.0 equiv) were added to a 250 mL round-bottom flask along with ∼25 mL of DMF. The mixture was heated to 95 °C and allowed to stir for 21 h. The flask was then allowed to cool to room temperature, and the reaction mixture was diluted with 100 mL of DI water. Product was then extracted with diethyl ether (4 × 50 mL), and the ether extracts were collected. Extracts were dried over anhydrous sodium sulfate (Na_2SO_4) and decanted into a clean flask. Solvent was then removed, and the product was recrystallized from ethanol. Product was filtered with suction as a white crystalline solid and dried under high vacuum for 8 h.

*Deprotection to n-Octadecylamine (**2**).* ^{15}*N*-Octadecyl phthalimide (1.84 g, 4.61 mmol, 1.0 equiv) and 0.71 mL of 51% hydrazine hydrate (11.5 mmol, 2.5 equiv) were added to a 250 mL round-bottom flask along with 75 mL of ethanol. The mixture was heated to reflux and allowed to stir for 5 h. Upon cooling to room temperature, the resulting precipitate was filtered off and washed repeatedly with DCM. Solvent was removed, and product was redissolved in DCM. The solution was then washed with 6 M NaOH (2 × 100 mL) and Brine (1 × 100 mL). The organic layer was then collected, dried over anhydrous Na_2SO_4, and decanted into a clean flask. Solvent was removed again via rotatory evaporation, and solid was collected and dried under high vacuum to afford pure product as a white solid.

*Synthesis of ^{15}N-Labeled 1-Napthylisothiocyanate (**4**).* Thiophosgene (0.64 mL, 6.35 mmol, 1.2 equiv) was added to a 250 mL round-bottom flask along with 25 mL of DCM, and the reaction mixture was cooled to 0 °C in an ice bath. ^{15}N-enriched 1-naphthylamine (1.01 g, 6.99 mmol, 1.0 equiv) and triethylamine (TEA) (3.86 mL, 27.9 mmol, 4.0 equiv) were dissolved in 15 mL of DCM in an addition funnel. The amine solution was then added dropwise into the cold, stirring solution of thiophosgene. When the amine solution was completely added, the ice bath was removed and the solution was allowed to stir at room temperature for an additional 2.5 h. The solution was then washed with brine (2 × 50 mL) and dried over anhydrous sodium sulfate. The mixture was decanted into a clean flask, and solvent was removed via rotatory evaporation. Product was then further purified by column chromatography (DCM as mobile phase) and collected as a yellow solid. Product was then dried under high vacuum for 4 h.

*Formation of Asymmetric Ureas and Thioureas (**5** and **7**).* The specific amounts of reagents, yields, NMR data, MS data, and FTIR data for each asymmetric urea are reported in the Supporting Information.

The amine (1.0−1.2 equiv) was added to a 250 mL round-bottom flask along with a stir bar and 70 mL of $CHCl_3$. The mixture was allowed to stir for 15 min prior to addition of the corresponding isocyanate/isothiocyanate (1.0−1.2 equiv). The reaction mixture was then allowed to stir at room temperature when employing alkyl amines or heated to reflux when employing aryl amines. In both cases, the solution was allowed to stir for 10−15 h. Upon completion, solvent was removed under reduced pressure and crude product was recrystallized from ethanol. The product, typically a white powder, was filtered and washed with ice-cold ethanol repeatedly. The solid was then collected and dried under high vacuum.

*Synthesis of ^{15}N-Labeled Carbodiimide Monomers (**6** and **8**).* Specific amounts of reagents, yields, NMR data, MS data, and FTIR data are reported in the Supporting Information. ^{15}N NMR data was not collected on any of the carbodiimide monomers due to greater than 90 s delay times.

Dibromotriphenylphosphorane (PPh_3Br_2, 1.2 equiv) was added to a round-bottom flask along with ∼5 mL of DCM. The reaction flask was then placed under N_2 atmosphere and cooled to 0 °C in an ice bath. TEA (2.5 equiv) was then added to the stirring mixture, and resulting vapors were allowed to dissipate. ^{15}N-labeled urea/thiourea (1.0 equiv) was then added to the mixture, and the solution was allowed to stir until completion (ca. 1−10 h) with the reaction progress monitored by IR spectroscopy. Upon completion, the reaction was quenched with ∼300 mL of pentane and the resulting precipitate was filtered and washed with additional pentane. Filtrate was collected, and solvent was removed via rotatory evaporation. This quenching process was repeated twice more to remove most of the byproducts from the system. Product was further purified by column chromatography (DCM as mobile phase) and collected. Solvent was removed, and the monomer was dried under high vacuum to afford pure product.

Polymerization of Carbodiimides with Ti(IV) Catalysts. All polymerizations were conducted in an inert N_2 atmosphere drybox. All glassware and solvents were dried prior to use for any polymerizations. Polymerization times vary greatly depending on the nature of the monomer used. The preweighed amount of catalyst was added directly to the monomer for solvent-free polymerizations. For solution-based polymerizations, the specified amount of catalyst was weighed out in a clean, dry vial and a catalyst solution was formed in dry $CHCl_3$. The necessary amount of catalyst solution was then injected into the reaction vial containing the monomer and allowed to stir for the allotted amount of time (see Supporting Information). To form optically active polymers with a helical

dx.doi.org/10.1021/ja4098803 | J. Am. Chem. Soc. 2013, 135, 19292−19303

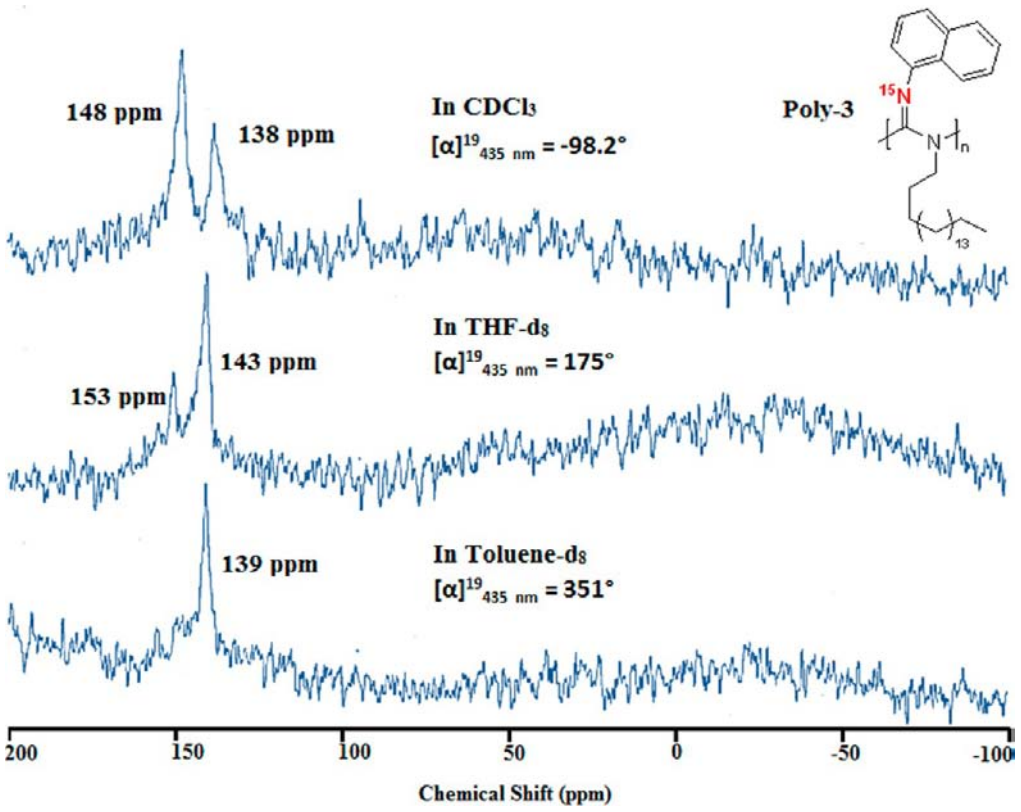

Figure 3. ^{15}N NMR spectra of **Poly-3** in $CDCl_3$, THF-d_8, and toluene-d_8 with corresponding specific values OR (c = 2.00 mg/mL, λ = 435 nm, T = 19 °C) in each solvent.

bias, **Cat-1**(R) and **Cat-1**(S) was utilized for chiral induction upon polymerization of all polymers. All polymers were worked up by redissolving the crude product in a minimal amount of chloroform and precipitating the pure product upon addition to methanol, a typical antisolvent. Polymer product was then filtered, collected, and dried under high vacuum. The monomer-to-catalyst ratio, yield, ^{1}H NMR, IR, and ^{15}N NMR data of each polymer are reported in the Supporting Information as well as scans of the IR spectra.

^{15}N NMR Collection of Precursor Compounds and Polymers. ^{15}N NMR collection of the polymers and precursor compounds was achieved using the same procedure previously reported.[48,49] Each spectrum was referenced externally to ^{15}N-enriched benzamide set to δ = 0.00 ppm. For the specific procedure of spectra acquisition see the Supporting Information.

RESULTS AND DISCUSSION

Preparation of the mono- and dilabeled polymers, **Poly-3** and **Poly-5**, is displayed in Scheme 1. Molecular weight (MW) determination for **Poly-3**, **-4**, and **-5** via gel permeation chromatography (GPC) was performed with an additive, *N,N*-dimethylethylenediamine, in order to reduce the affinity of the nitrogen-rich backbone to the stationary phase of the column. The number-average MW (M_n), weight-average MW (M_w), and polydispersity (PDI) for the newly reported polymers are as follows: (a) **Poly-3**, M_n = 79 000 Da, M_w = 200 000 Da, PDI = 2.53; (b) **Poly-4**, M_n = 34 000 Da, M_w = 81 000 Da, PDI = 2.38; (c) **Poly-5**, M_n = 60 000 Da, M_w = 140 000 Da, PDI = 2.33. Variable-temperature polarimetry of **Poly-3** displays a similar profile to the chiroptical switching reported by Kennemur et al. albeit with slightly diminished amplitude (see Supporting Information).

Effect of Solvent on ^{15}N NMR Spectra of Poly-3. Taking another look at the C═N imine stretch in the IR spectra of **Poly-3** reveals an interesting result. As previously stated, the IR spectrum of the polymer dissolved in $CHCl_3$ displays two peaks in the imine C═N region. In this solvent, the peak at 1619 cm^{-1} appears larger in intensity than the lower wavenumber peak in the region at 1602 cm^{-1}. These two peaks were first attributed to regioirregular placement of the pendant groups along the polymer backbone but was later disproven by VT-FTIR.[53] It is noteworthy to point out that two peaks corresponding to the imine nitrogen are lower in wavenumber than the values reported by Kennemur et al. (ca. 21 and 16 cm^{-1}, respectively).[43,53] This is attributed to the significant ^{15}N-isotope shift experienced by the imine stretch in the IR spectra upon specific isotope labeling. When **Poly-3** is dissolved in THF, however, the two peaks switch in intensities and the peak at 1602 cm^{-1} becomes more pronounced, further disproving regioirregularity. Switching the solvent to toluene results in complete disappearance of the peak at 1619 cm^{-1}, leaving a single stretch at 1601 cm^{-1} corresponding to the imine bond. These are the same peaks that change in intensity as a function of temperature.

Quantification of the populations of the two states is not possible using IR spectroscopy because of the substantial overlap present. Hence, we turned to ^{15}N NMR to further confirm the proposed two-state model and quantify their relative populations. ^{15}N NMR spectra of **Poly-3** dissolved in $CDCl_3$ (top), THF-d_8 (middle), and toluene-d_8 (bottom) are shown in Figure 3. A similar trend to that observed in the IR spectra of the polymer dissolved in each solvent is seen in the

dx.doi.org/10.1021/ja4098803 | J. Am. Chem. Soc. 2013, 135, 19292−19303

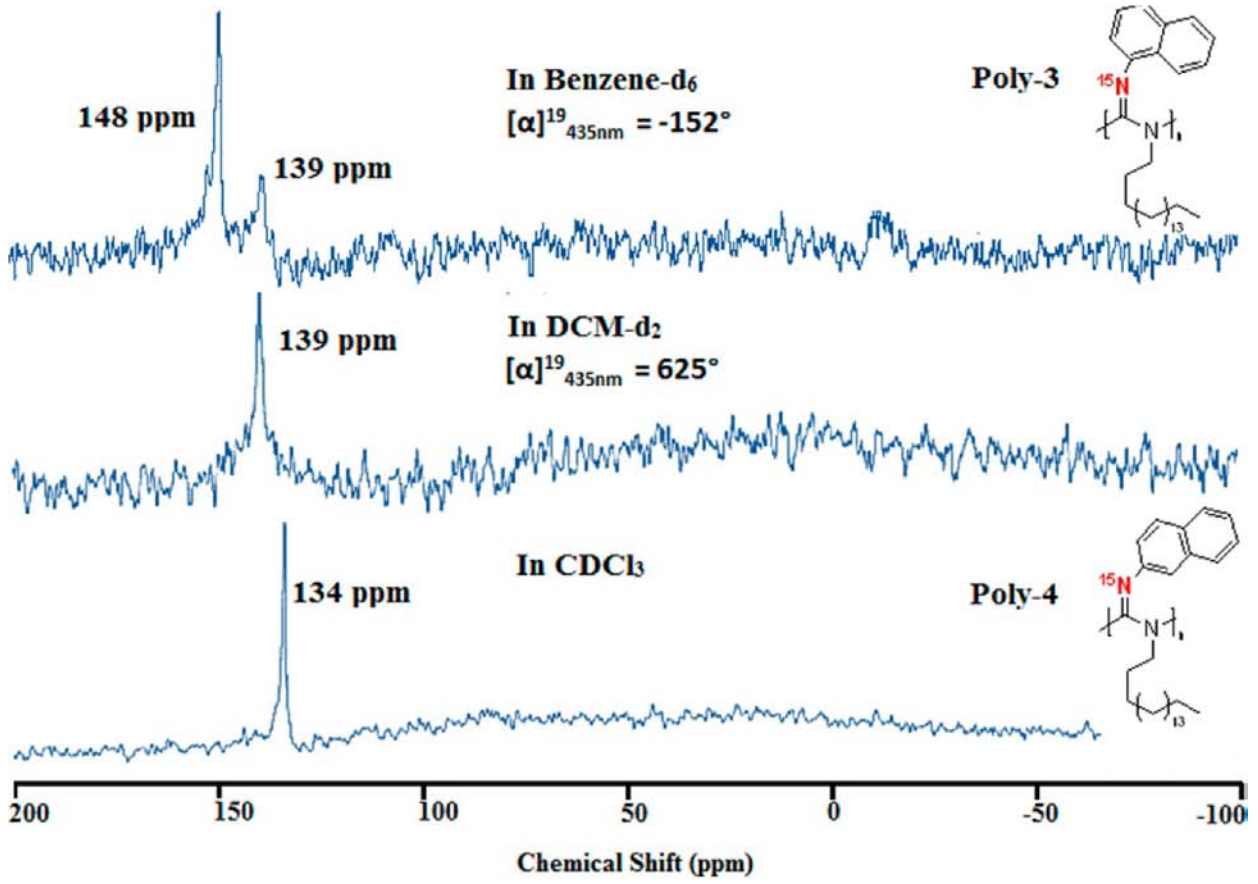

Figure 4. ^{15}N NMR spectra of **Poly-3** in DCM-d_2 and benzene-d_6 displays predominantly one peak in each, albeit the opposite, signifying that the majority of the polymer chains are in a single conformation. Spectrum of **Poly-4** in $CDCl_3$ displays one peak unlike the very similar **Poly-3,** verifying that when chiroptical switching is removed there is the presence of two specific conformations.

^{15}N NMR spectra. In $CDCl_3$, two peaks are present with the peak at δ = 148 ppm being the predominant chemical shift in the spectra and the relative integration of each peak equal to about 2:1. In THF-d_8, both peaks are shifted slightly farther downfield and switch in intensities with the relative integration of the peaks at δ = 153 and 143 ppm equal to about 1:2, respectively. In toluene-d_8, the downfield peak is nearly completely eliminated with one peak at δ = 139 ppm in the imine region. The polymer is still regioregular since both ^{15}N NMR peaks correspond to the imine nitrogen. Both the IR and the ^{15}N NMR peaks corresponding to the imine nitrogen appear to be directly associated with the polymer conformation leading to the different specific OR measured. High positive OR values correlate to the upfield peak in the ^{15}N NMR and the IR stretch at 1602 cm^{-1} (state A), whereas the downfield peak and the peak at 1619 cm^{-1} correlate to the lower negative values (state B). This data supports our hypothesis that the switching process occurs in a concerted fashion between two states with the observed OR changes resulting from the equilibrium populations of these two distinct conformations. Chemical shifts of both states remain relatively constant in all three solvents, supporting the polymer chains adopting largely similar conformations in each solvent. It is also noted that the rate of switching between these two states is very rapid when compared to the NMR time scale, so measuring the kinetics of the switching process is not possible using this technique.

Chloroform, THF, and toluene were found to be the most versatile solvents for the chiroptical switching process in this polymer system, so they were the natural choice for these inaugural NMR studies. In an attempt to establish the population extremes of the system, multiple solvents were studied to determine which solvents provide the maximum positive values and minimum negative values of OR. At room temperature, dichloromethane was found to provide the highest specific OR, ca. $[\alpha]^{22}_{435\ nm}$ = 625°, while benzene provided the lowest value, ca. $[\alpha]^{22}_{435\ nm}$ = −152°, of the solvents tested. The specific OR of **Poly-3** in DCM and benzene, however, does not vary greatly as a function of temperature and never passes through 0° at all feasible temperatures. ^{15}N NMR of the polymer in DCM-d_2 displays one peak corresponding to the imine nitrogen at δ = 139 ppm, which agrees with the trend between the vast majority of the polymer chains adopting state A at higher positive specific OR values. Also, in concurrence with the observed trends, the spectrum in benzene-d_6 displays predominantly one peak at δ = 148 ppm. This suggests that the vast majority of the naphthyl pendant groups attached to the imine nitrogen are in a single conformation in both DCM and benzene, albeit opposite from one another. In addition, the chemical shifts of the two distinct states remained constant in both benzene-d_6 and DCM-d_2, further supporting the hypothesis that the two conformations are the same in all solvents. It should be noted that the higher field peak at ca. 138 ppm never fully disappears, and whether this is a "non-responsive" portion of the polymer chains or an inability to uncover conditions allowing for full negative OR values remains to be seen.

dx.doi.org/10.1021/ja4098803 | J. Am. Chem. Soc. 2013, 135, 19292−19303

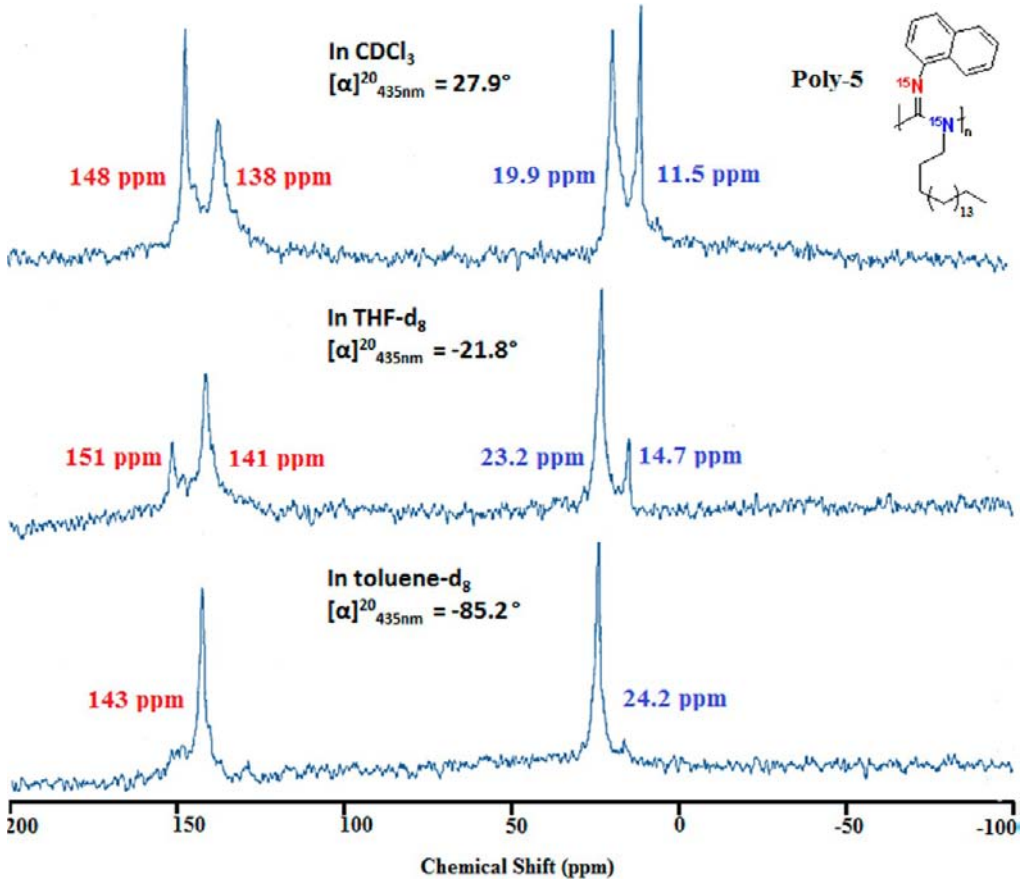

Figure 5. ^{15}N NMR spectra of **Poly-5** in $CDCl_3$, THF-d_8, and toluene-d_8 at 20 °C showing the effect of the chiroptical switching phenomenon on the amine nitrogen.

The chiroptical switching properties of the polymer are completely removed upon changing the connectivity of the naphthyl pendant group as evident by switching the imine connection from the 1 position to the 2 position of the ring.[43] For this reason, poly(^{15}*N*-(2-naphthyl)-*N*-octadecylcarbodiimide) (**Poly-4**) was synthesized using the original protocol designed by DeSousa et al.[48] ^{15}N NMR spectra of **Poly-4** in $CDCl_3$ displayed only one peak in the imine region unlike the very similar, but differently connected, **Poly-3**. Also, the peak is shifted farther upfield close to the ^{15}N NMR chemical shift of poly(^{15}*N*-phenyl-*N*-hexylcarbodiimde), suggesting that **Poly-4** is closer conformationally to this polymer rather than **Poly-3**. This suggests that the presence of two conformations is a function of the attachment of the naphthyl ring just like the optical rotation dependence on solvent and temperature. ^{15}N NMR spectra of **Poly-4** in $CDCl_3$ and **Poly-3** in DCM-d_2 and benzene-d_6 are shown in Figure 4.

Effect of Switching Process on the Amine Nitrogen. The chiroptical switching process is known to have a great deal of effect on the imine nitrogen and its environment. It is still unclear, however, whether the amine nitrogen is affected by the switching process. To probe the effect of the process on the amine nitrogen, a new synthesis scheme was created to produce the dilabeled poly(^{15}*N*-(1-naphthyl)-^{15}*N*-octadecylcarbodiimide) (**Poly-5**). The enantiomer of the catalyst used for polymerization of **Poly-3** was employed to ensure that the opposite handed helix of **Poly-5** formed upon polymerization would not affect the presence of the peaks in the imine region of the ^{15}N NMR. The specific OR profiles of **Poly-5** reversed compared to **Poly-3** (see Supporting Information), confirming the opposite handed helix was formed upon polymerization. The synthesis scheme for **Poly-5** is shown in Scheme 1. The initial ^{15}N NMR spectra were collected in the same solvents as in studies of **Poly-3** ($CDCl_3$, THF-d_8, and toluene-d_8 in Figure 5).

The resulting peaks corresponding to the imine nitrogen of **Poly-5** mimicked the peaks seen in the spectra of **Poly-3** with the same pattern seen in all three solvents. The amine nitrogen also displayed two peaks in a mirror image of the imine nitrogen chemical shifts. In $CDCl_3$, the peak at δ = 148 ppm for imine nitrogen and the peak at δ = 11.5 ppm corresponding to the amine nitrogen predominate in the spectra where the peaks at δ = 138 and 19.9 ppm correlate with the minority population of polymer chains. The spectrum in THF-d_8 continues the trend with the intensities of both sets of peaks switching. Another interesting observation is the shift downfield of all four peaks. This was also observed in the spectrum of **Poly-3**, where the two imine nitrogen chemical shifts migrate downfield a total of 5 ppm. This can most likely be attributed to some specific solvent−backbone interaction that adds to the magnetic shielding of the backbone nitrogens. In toluene-d_8, the peaks are also shifted slightly downfield. This observation differs from the peak identified in the imine region of **Poly-3** in toluene-d_8 in which the peak corresponding to the imine nitrogen is located at δ = 139 ppm. The source of this observation is still unknown and under further investigation. The populations of polymer conformations, however, correlate perfectly with the expected trend seen with **Poly-3**. The peaks δ = 151 and 14.7

dx.doi.org/10.1021/ja4098803 | J. Am. Chem. Soc. 2013, 135, 19292−19303

ppm are nearly completely diminished with only one peak in both the imine and the amine regions.

Using Variable-Temperature ^{15}N NMR To Measure the Thermodynamics of Switching. In addition to changing the solvent composition of dilute polymer solutions, altering the temperature in solutions of **Poly-3** and **Poly-5** causes the specific OR and CD to vary drastically in a reversible fashion. As expected, variable-temperature ^{15}N NMR provided further insight into how the populations of each specific polymer conformation are modulated as a function of temperature. ^{15}N NMR spectra at 20, 30, 45, and 60 °C in toluene-d_8 are displayed in Figure 6. When the temperature is increased and

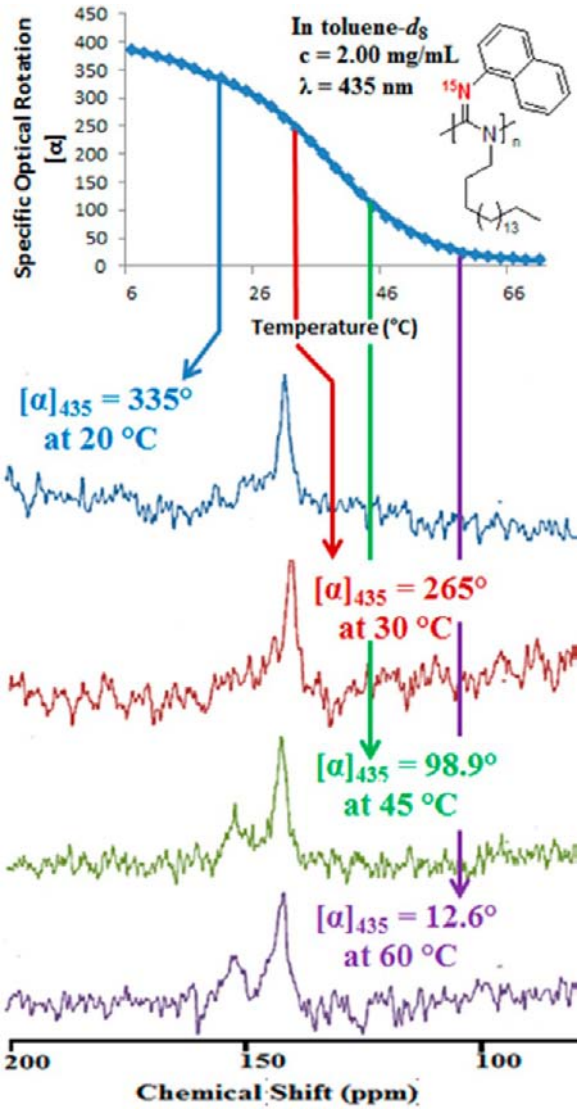

Figure 6. Variable-temperature ^{15}N NMR spectra of **Poly-3** in toluene-d_8 at 20, 30, 45, and 60 °C showing the conformational dependence on the temperature of the polymer solution.

the specific OR of the polymer sample decreases the intensity of the peak at δ =152 ppm slowly increases, suggesting that the population of the secondary conformation corresponding to the downfield chemical shift is also increasing. At 45 °C, the relative integration of the downfield peak and the peak at δ = 142 ppm reveals a ∼1:2 ratio, which mimics the polymers behaviors in THF at room temperature. The specific OR of the polymer in toluene at 45 °C is 98.9°, slightly less than the polymer in THF (ca. $[\alpha]^{19}_{435}$ = 175°), so the slightly increased prominence of the downfield peak correlates with the trend. At 60 °C, the trend continues the conformation population analogous to the downfield peak growing in intensity integrating relative to the upfield chemical shift to 1:1.5, respectively. In all solvents, state B is populated with increasing abundance as temperatures increase as evident by the ^{15}N chemical shift at ca. 150 ppm and the negative specific OR values.

VT-^{15}N NMR spectra of **Poly-3** and **Poly-5** in THF-d_8 are significantly different with the populations of each conformation altering much more drastically than in toluene-d_8 (see Supporting Information). To observe the most significant alterations of the polymer conformation in THF, temperatures of 20, 30, and 40 °C were chosen for variable-temperature studies. At 20 °C, the upfield chemical shift in the ^{15}N NMR spectrum of **Poly-3** predominates significantly with the relative integration of the downfield peak with respect to the upfield peak equal to about 1:2.2. Increasing the temperature of the NMR solution to 30 °C results in an increase in the relative population of the downfield chemical shift at 151 ppm and a decrease in the specific OR from $[\alpha]^{20}_{435}$ = 175° to $[\alpha]^{30}_{435}$ = −2.0°. Further heating the solution to 40 °C causes the specific OR to reach the minimum value in THF of $[\alpha]^{40}_{435}$ = −55° and the relative ratio of the downfield peak to the upfield peak equal to about 1:1.1. Interestingly, the populations of each **Poly-3** conformation never favor the state corresponding to the downfield shift in THF similar to when dissolved in toluene-d_8; however, the population change is slightly more significant.

In $CDCl_3$, the VT-^{15}N NMR spectra display a considerably more pronounced population change over a smaller range of temperatures when compared to toluene-d_8 and THF-d_8 (Figure 7). At 0 °C, the specific OR of **Poly-3** is at the maximum value (ca. $[\alpha]^{19}_{435}$ = 418°) in this particular solvent. ^{15}N NMR analysis at this temperature reveals a single peak in the spectra matching nicely with the trend seen in previous spectra. The conformation corresponding to the downfield shift grows significantly in population with respect to the upfield peak upon heating the polymer solution to 10 °C with relative integrations of the two peaks equal to about 1:2. The downfield conformation becomes even more prominent when the temperature is increased further to 15 °C. At 20 °C, the equilibrium shifts in favor of the conformation corresponding with the downfield shift with the relative integrations of the two peaks equal to ∼1.2:1. VT-^{15}N NMR spectra of **Poly-5** in toluene-d_8, THF-d_8, and $CDCl_3$ mimic the spectra collected for **Poly-3** in the same solvents (see Supporting Information). This data continues to match nicely with the observed trend between the chiroptical changes and the population change of two distinct conformations.

Since we can now quantify the specific proportions of each polymer conformation in solution at different temperatures, it is now possible to calculate the change in enthalpy and entropy during the equilibrium process. This can be accomplished using the van't Hoff relationship shown below in eq 1 where K_{eq} is the equilibrium constant, R is the gas constant (1.989 cal/(mol·K)), and T is the temperature in Kelvin. This method is used extensively to study biological macromolecular systems in order to examine specific functions and dynamic behavior in DNA and peptides.[54,55]

$$\ln(K_{eq}) = -\frac{\Delta H_{switching}}{RT} + \frac{\Delta S_{switching}}{R} \quad (1)$$

dx.doi.org/10.1021/ja4098803 | J. Am. Chem. Soc. 2013, 135, 19292−19303

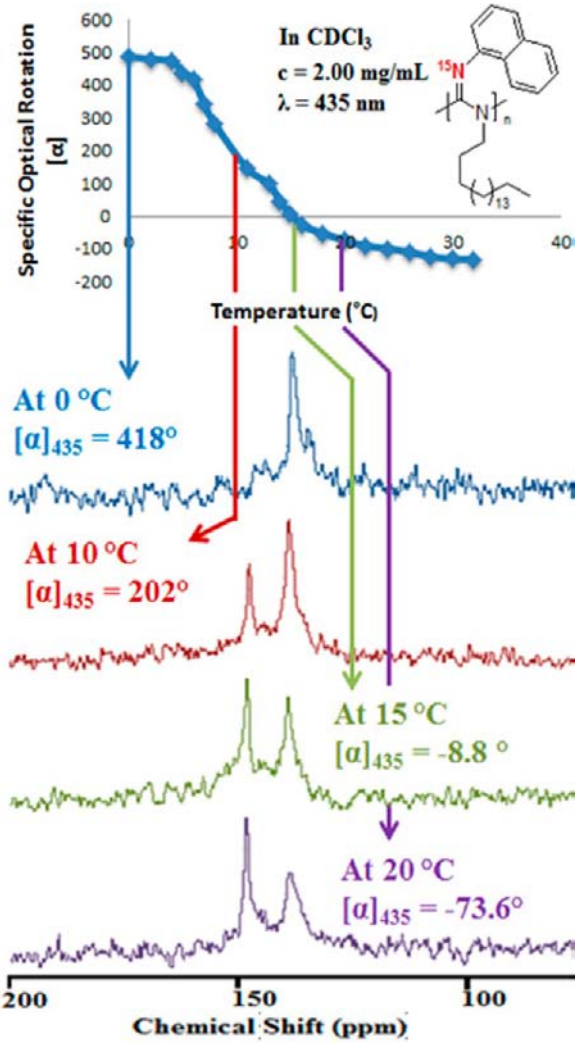

Figure 7. Variable-temperature ^{15}N NMR spectra of **Poly-3** in $CDCl_3$ at 0, 10, 15, and 20 °C displaying the distinct population shifts as the temperature of the solution is altered.

For our system where the equilibrium consists of interconversions of two specific states, the relative integrations of the peaks in the ^{15}N NMR spectra at various temperatures allows for a qualitative measure of the specific proportions of each conformation in solution. With these proportions, one can now calculate K_{eq} simply by dividing the relative concentration of state B by the relative concentration of state A (i.e., K_{eq} = [B]/[A]). Plotting the values of $\ln(K_{eq})$ vs $1/T$ should result in a linear plot with the slope equal to $-\Delta H_{eq}/R$ and the y intercept equal to $\Delta S_{eq}/R$. Results of this analysis are shown in Figure 8.

This analysis provides consistent results between different batches of identical polymers. Results of the van't Hoff analysis and errors associated to the error of integration for both **Poly-3** and **Poly-5** are outlined in Table 1. van't Hoff plots for **Poly-5** match up very well with the plots of **Poly-3** providing similar energy values, further substantiating the validity of this analysis.

These polymers display positive enthalpy changes in all solvents indicating that we are populating a higher energy state as the conformations are shifted from state A to state B. Interestingly, both **Poly-3** and **Poly-5** have the highest observed $\Delta H_{switching}$ when dissolved in $CHCl_3$ despite the entire switching process occurring below room temperature.

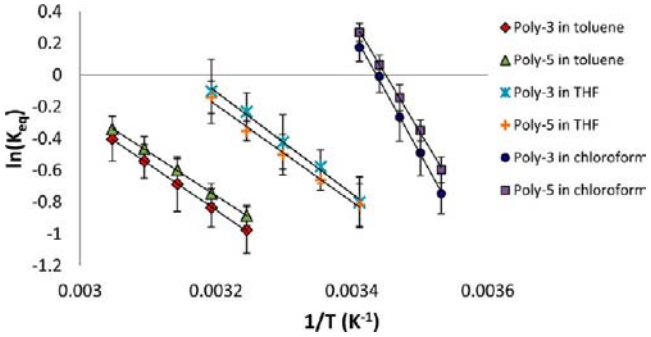

Figure 8. van't Hoff plot of **Poly-3** and **Poly-5** in toluene-d_8, THF-d_8, and $CDCl_3$ used to determine the thermodynamics of the chiroptical switching process.

This is due to the larger quantity of polymer chains occupying the higher energy state B compared to the switching process in toluene. The driving force behind this phenomenon is the very large entropy change associated with the switching in $CHCl_3$. The increase in the enthalpies and entropies of switching for both polymers when the solvent is changed from toluene to THF to chloroform implies that the change in disorder of the system (polymer and solvent) is substantially larger when the polymer is dissolved in $CHCl_3$. If we assume that the entropy change associated with the specific molecular motion of the polymer will be the same in all solvents then the large difference in $\Delta S_{switching}$ could be attributed to increased disorder in the chloroform solvent molecules as the polymer undergoes the switching process. This assumption is reasonable since both conformations present in solution are the same or very similar in all three solvents as evident by the comparable chemical shift values. This is most likely due to ordered solvent−polymer interactions between the chloroform solvent molecules and the polymer chains adopting state A. As switching from state A to state B occurs, the solvent−polymer ordering becomes less, thus increasing the entropy of the system. An even stronger solvent−polymer ordered interaction in toluene causes the switching process to become less favorable and, in turn, inhibits the polymer chains from predominantly adopting the higher energy state B. We propose that the toluene solvent molecules may associate with the polymer chains more favorably with respect to $CHCl_3$ through ordered $\pi-\pi$ stacking between the solvent and the naphthyl pendant groups. Due to this increasingly ordered interaction, the switching phenomenon from state A to state B is much less favorable in toluene due to the diminished propensity of the toluene molecules to dissociate upon switching. This hypothesis supports the higher observed switching temperatures of **Poly-3** and **Poly-5** in toluene as well as the limited number of polymer chains adopting state B.

Although absolute identification of the conformational reorientation cannot be unambiguously determined via ^{15}N NMR, new insights can be drawn from the calculated energy parameters, furthering the understanding of this dynamic equilibrium. Herein, we propose two hypothesized pendant group conformations (Figure 9) believed to be the two observed states visible in the ^{15}N NMR spectra of **Poly-3** and **Poly-5**. The naphthyl pendant group in the proposed; lower energy state A is positioned out of the plane of the backbone imine allowing for no p-orbital overlap between the conjugated naphthyl ring and the imine π bond. Upon switching, the naphthyl ring is hypothesized to reorient in plane with the

dx.doi.org/10.1021/ja4098803 | J. Am. Chem. Soc. 2013, 135, 19292−19303

Table 1. Empirically Calculated van't Hoff Enthalpies and Entropies of the Reversible, Chiroptical Switching Process Using the Relative Integration the Nitrogen-15 NMR Peaks Corresponding to the Imine Nitrogen To Measure the Populations of Each Polymer Conformation

	Poly-3			Poly-5		
solvent	toluene	THF	chloroform	toluene	THF	chloroform
specific OR changes[a]	15−375°	−50−406°	−132−488°	−99−3°	−99−30°	−76−46°
$\Delta H_{switching}$ (kcal/mol)	5.8 (±2.9)	6.4 (±3.3)	15 (±3.4)	5.5 (±1.4)	6.1 (±2.2)	14 (±2.4)
$\Delta S_{switching}$ (cal·mol^{-1}·K^{-1})	17 (±9.0)	20 (±11)	53 (±12)	16 (±4.5)	19 (±7.5)	49 (±8.3)
$\Delta G_{switching}$ at 25 °C (kcal/mol)[b]	+0.77	+0.36	−0.37	+0.71	+0.40	−0.39

[a]All specific OR measurements recorded for 2.00 mg/mL dilute; polymer solutions at 435 nm. [b]Free energy of switching estimated using the van't Hoff enthalpies and entropies.

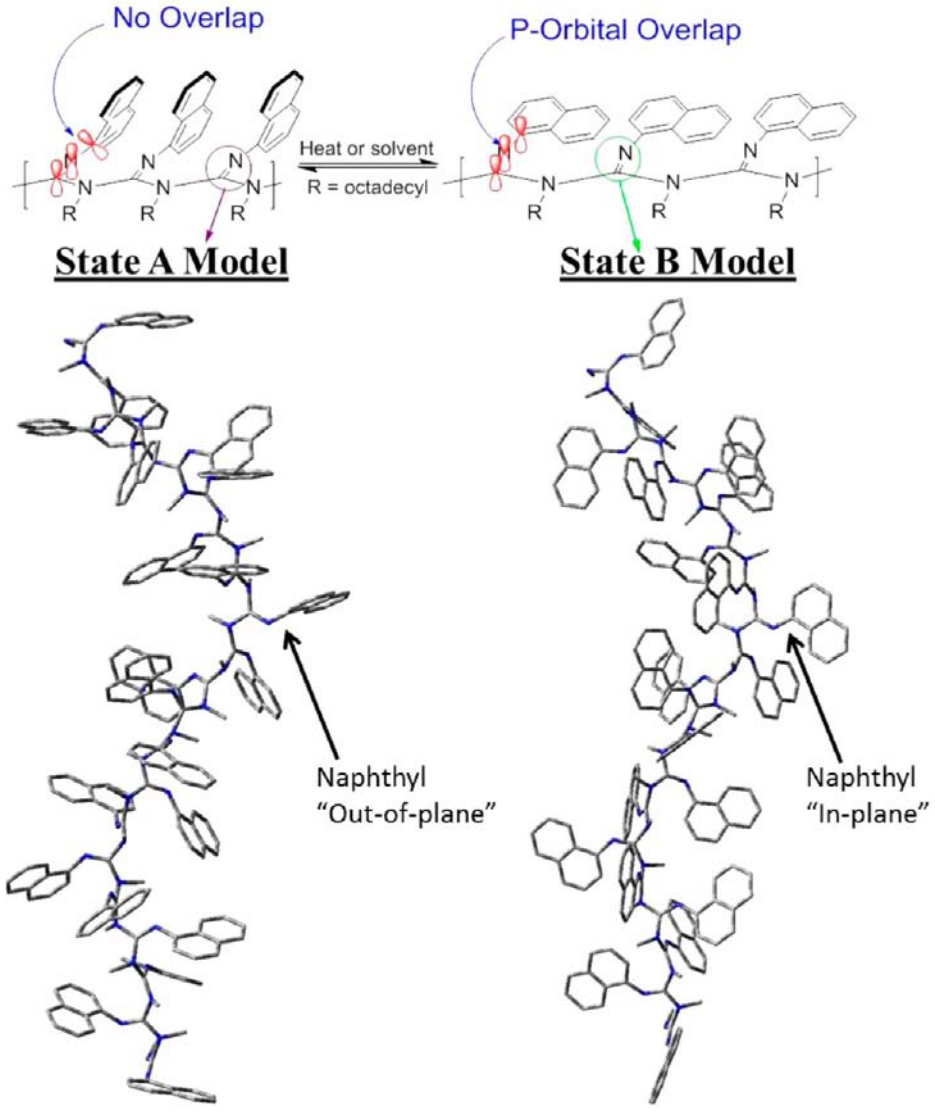

Figure 9. Proposed conformational structures of states A and B represented in chemical structures, and optimized 24mer model showing the hypothesized naphthyl orientations in and out of plane of the backbone imine nitrogen.

backbone imine, allowing for conjugation to occur. This state also correlates with the higher energy state B due to the added steric interactions between adjacent aryl pendant groups. Currently, new studies are underway to pinpoint the exact pendant group orientations using VCD spectroscopy coupled with density functional theory (DFT) calculations.

The free energy of the switching process was then estimated using the van't Hoff energies measured for **Poly-3** and **Poly-5** (Table 1). The positive free energy values for both polymers in toluene and THF match nicely with the higher switching temperatures of the polymers in both solvents and the fact that the equilibrium never shifts in favor of state B at any temperature observed. In addition, the estimated free energy of switching for **Poly-3** and **Poly-5** in chloroform reveals negative $\Delta G_{switching}$, which is also in concurrence with the observed trend due to the entire switching process occurring

dx.doi.org/10.1021/ja4098803 | J. Am. Chem. Soc. 2013, 135, 19292−19303

below room temperature and the equilibrium shifting in favor of the downfield conformation at temperatures greater than 18 °C. This new data offers new insight in what has proven to be an intensely interesting polymer behavior.

CONCLUSIONS

Synthesis of ^{15}N-labeled poly(^{15}*N*-1-naphthyl-*N*-octadecylcarbodiimide) (**Poly-3**) and poly(^{15}*N*-1-naphthyl-^{15}*N*′-octadecylcarbodiimide) (**Poly-5**) has provided ample new understanding on the driving forces behind the solvent effects of chiroptical switching process. We discovered evidence suggesting that the process occurs in a two-state model and the populations can be determined using ^{15}N NMR spectroscopy. The changes in specific OR results from a rapid equilibrium between these two states and the position of equilibrium is a function of both solvent and temperature. We further propose that the two conformations are similar in all solvents, but the large alterations in entropy are related to the disorder of the solvents in the solvation sphere during the switching process. These populations were found to possess potent temperature and solvent dependence in all cases studied. Using variable-temperature ^{15}N NMR to measure the proportions of the polymer chains in each specific conformation, we were able to calculate the van't Hoff enthalpies and entropies of switching. This analysis provided different values for chloroform and toluene associated with significantly larger changes in entropy when the switching process occurs in chloroform. The additional order of the system in toluene has contributions from ordering of the local solvent molecules in some specific manner around the polymer chains (possibly $\pi-\pi$ interactions between the toluene and the naphthyl pendant group). These added interactions are believed to be the root of the higher switching temperatures as well as the limited number of polymer chains adopting state B in toluene. In addition, the free energy of switching was calculated for both polymer systems, showing that $\Delta G_{switching}$ is positive in toluene and negative in chloroform at 25 °C. This also correlates with the trend due to the switching process occurring below room temperature in chloroform and above room temperature in toluene. To further elucidate the mechanism of the chiroptical switching process, VCD measurements and calculations are currently ongoing to help identify the conformations present in the system.

ASSOCIATED CONTENT

Supporting Information

Further experimental characterization on all precursor compounds and polymers including NMR, IR, specific OR, and mass spectral data. This material is available free of charge via the Internet at http://pubs.acs.org.

AUTHOR INFORMATION

Corresponding Author

E-mail: Bruce.novak@utdallas.edu

Notes

The authors declare no competing financial interest.

ACKNOWLEDGMENTS

Funding for this work was provided by the Faculty start-up fund from the University of Texas at Dallas (UTD), the Endowed Chair for Excellence at UTD, and the Howard Schaeffer Distinguished Chair at NCSU. Our special thanks to Dr. Sabapathy Sankar (NCSU) and Dr. Hien Nguyen (UTD) for their aid in NMR acquisition. We thank Dr. Dennis Smith (UTD) and Ben Batchelor (UTD) for their help in the MW determination of the reported polymers via GPC. We gratefully acknowledge the NSF-MRI grant (CHE-1126177) used to purchase the Bruker Advance III 500 NMR instrument. We thank the NCSU Department of Chemistry Mass Spectrometry Facility funded by the North Carolina Biotechnology Center and NCSU Department of Chemistry for all mass spectral data collected.

REFERENCES

(1) Agati, G.; McDonagh, A. F. *J. Am. Chem. Soc.* **1995**, *117*, 4425−4426.
(2) Suk, J.-m.; Naidu, V. R.; Liu, X.; Lah, M. S.; Jeong, K.-S. *J. Am. Chem. Soc.* **2011**, *133*, 13938−13941.
(3) Zou, G.; Jiang, H.; Zhang, Q.; Kohn, H.; Manaka, T.; Iwamoto, M. *J. Mater. Chem.* **2010**, *20*, 285−291.
(4) Canary, J. W.; Mortezaei, S.; Liang, J. *Coord. Chem. Rev.* **2010**, *254*, 2249−2266.
(5) Li, D.; Wang, Z. Y.; Ma, D. *Chem. Commun.* **2009**, 1529−1531.
(6) Zhang, G.; Liu, M. *J. Mater. Chem.* **2009**, *19*, 1471−1476.
(7) Feringa, B.; Wynberg, H. *J. Am. Chem. Soc.* **1977**, *99*, 602−603.
(8) Murata, K.; Aoki, M.; Nishi, T.; Ikeda, A.; Shinkai, S. *Chem. Commun.* **1991**, 1715−1718.
(9) Yamaguchi, T.; Uchida, K.; Irie, M. *J. Am. Chem. Soc.* **1997**, *119*, 6066−6071.
(10) Feringa, B. L.; van, D. R. A.; Koumura, N.; Geertsema, E. M. *Chem. Rev.* **2000**, *100*, 1789−1816.
(11) Effing, J. J.; Kwak, J. C. T. *Angew. Chem., Int. Ed. Engl.* **1995**, *34*, 88−90.
(12) Ikeda, T.; Tsutsumi, O. *Science* **1995**, *268*, 1873−1875.
(13) Yamazaki, I.; Ohta, N. *Pure Appl. Chem.* **1995**, *67*, 209−216.
(14) Oosterling, M. L. C. M.; Schoevaars, A. M.; Haitjema, K. J.; Feringa, B. L. *Isr. J. Chem.* **1997**, *36*, 341−348.
(15) Ueno, A.; Takahashi, K.; Anzai, J.; Osa, T. *J. Am. Chem. Soc.* **1981**, *103*, 6410−6415.
(16) Mammana, A.; Carroll, G. T.; Areephong, J.; Feringa, B. L. *J. Phys. Chem. B* **2011**, *115*, 11581−11587.
(17) Pijper, D.; Jongejan, M. G. M.; Meetsma, A.; Feringa, B. L. *J. Am. Chem. Soc.* **2008**, *130*, 4541−4552.
(18) Green, M. M.; Peterson, N. C.; Sato, T.; Teramoto, A.; Cook, R.; Lifson, S. *Science* **1995**, *268*, 1860−1866.
(19) Gellman, S. H. *Acc. Chem. Res.* **1998**, *31*, 173−180.
(20) Cornelissen, J. J. L. M.; Rowan, A. E.; Nolte, R. J. M.; Sommerdijk, N. A. J. M. *Chem. Rev.* **2001**, *101*, 4039−4070.
(21) Hill, D. J.; Mio, M. J.; Prince, R. B.; Hughes, T. S.; Moore, J. S. *Chem. Rev.* **2001**, *101*, 3893−4012.
(22) Nakano, T.; Okamoto, Y. *Chem. Rev.* **2001**, *101*, 4013−4038.
(23) Lam, J. W. Y.; Tang, B. Z. *Acc. Chem. Res.* **2005**, *38*, 745−754.
(24) Yashima, E.; Maeda, K. *Macromolecules* **2008**, *41*, 3−12.
(25) Yashima, E.; Maeda, K.; Iida, H.; Furusho, Y.; Nagai, K. *Chem. Rev.* **2009**, *109*, 6102−6211.
(26) Kennemur, J. G.; Novak, B. M. *Polymer* **2011**, *52*, 1693−1710.
(27) Prest, P.-J.; Prince, R. B.; Moore, J. S. *J. Am. Chem. Soc.* **1999**, *121*, 5933−5939.
(28) Zhao, D.; Moore, J. S. *J. Am. Chem. Soc.* **2002**, *124*, 9996−9997.
(29) Banno, M.; Yamaguchi, T.; Nagai, K.; Kaiser, C.; Hecht, S.; Yashima, E. *J. Am. Chem. Soc.* **2012**, *134*, 8718−8728.
(30) Green, M. M.; Gross, R. A.; Crosby, C., III; Schilling, F. C. *Macromolecules* **1987**, *20*, 992−999.
(31) Lifson, S.; Green, M. M.; Andreola, C.; Peterson, N. C. *J. Am. Chem. Soc.* **1989**, *111*, 8850−8858.
(32) Nolte, R. J. M.; Van, B. A. J. M.; Drenth, W. *J. Am. Chem. Soc.* **1974**, *96*, 5932−5933.
(33) Van, B. A. J. M.; Nolte, R. J. M.; Naaktgeboren, A. J.; Zwikker, J. W.; Drenth, W.; Hezemans, A. M. F. *Macromolecules* **1983**, *16*, 1679−1689.

(34) Takei, F.; Yanai, K.; Onitsuka, K.; Takahashi, S. *Angew. Chem., Int. Ed.* **1996**, *35*, 1554−1556.
(35) Kwak, G.; Masuda, T. *J. Polym. Sci., Part A: Polym.Chem.* **2001**, *39*, 71−77.
(36) Aoki, T.; Kaneko, T.; Maruyama, N.; Sumi, A.; Takahashi, M.; Sato, T.; Teraguchi, M. *J. Am. Chem. Soc.* **2003**, *125*, 6346−6347.
(37) Ito, Y.; Ihara, E.; Murakami, M. *Angew. Chem., Int. Ed.* **1992**, *31*, 1509−1510.
(38) Ito, Y.; Ihara, E.; Murakami, M.; Sisido, M. *Macromolecules* **1992**, *25*, 6810−6813.
(39) Goodwin, A.; Novak, B. M. *Macromolecules* **1994**, *27*, 5520−5522.
(40) Kim, J.; Novak, B. M.; Waddon, A. J. *Macromolecules* **2004**, *37*, 1660−1662.
(41) Kim, J.; Novak, B. M.; Waddon, A. J. *Macromolecules* **2004**, *37*, 8286−8292.
(42) Tang, H.-Z.; Lu, Y.; Tian, G.; Capracotta, M. D.; Novak, B. M. *J. Am. Chem. Soc.* **2004**, *126*, 3722−3723.
(43) Kennemur, J. G.; Clark, J. B.; Tian, G.; Novak, B. M. *Macromolecules* **2010**, *43*, 1867−1873.
(44) Kennemur, J. G.; Kilgore, C. A.; Novak, B. M. *J. Polym. Sci., Part A: Polym. Chem.* **2011**, *49*, 719−728.
(45) Tang, H.-Z.; Boyle, P. D.; Novak, B. M. *J. Am. Chem. Soc.* **2005**, *127*, 2136−2142.
(46) Tang, H.-Z.; Novak, B. M.; He, J.; Polavarapu, P. L. *Angew. Chem., Int. Ed.* **2005**, *44*, 7298−7301.
(47) Jennings, W. B.; Boyd, D. R. *J. Am. Chem. Soc.* **1972**, *94*, 7187−7188.
(48) DeSousa, J. D.; Novak, B. M. *ACS Macro Lett.* **2012**, *1*, 672−675.
(49) Reuther, J. F.; D., D. J.; Novak, B. M. *Macromolecules* **2012**, *45*, 7719−7728.
(50) Kai, H.; Morioka, Y.; Koriyama, Y.; Okamoto, K.; Hasegawa, Y.; Hattori, M.; Koike, K.; Chiba, H.; Shinohara, S.; Iwamoto, Y.; Takahashi, K.; Tanimoto, N. *Bioorg. Med. Chem. Lett.* **2008**, *18*, 6444−6447.
(51) Wood, G. W. *J. Chem. Soc.* **1953**, 3327.
(52) Tian, G.; Lu, Y.; Novak, B. M. *J. Am. Chem. Soc.* **2004**, *126*, 4082−4083.
(53) Kennemur, J. G.; DeSousa, J. D.; Martin, J. D.; Novak, B. M. *Macromolecules* **2011**, *44*, 5064−5067.
(54) Ambrosone, L.; Ragone, R. *Int. J. Biol. Macromol.* **2000**, *27*, 241−244.
(55) Lavelle, L.; Fresco, J. R. *Nucleic Acids Res.* **1995**, *23*, 2692−2705.